Journal of Low Temperature Physics (2024) 217:383–392
https://doi.org/10.1007/s10909-024-03193-z

A Cryogenic Testbed for Polarization Modulators and Cryogenic Mechanisms

F. Columbro[1,2] · P. de Bernardis[1,2] · A. Coppolecchia[1,2] · E. Marchitelli[1,2] · S. Masi[1,2] · A. Occhiuzzi[1,2]

Received: 3 November 2023 / Accepted: 21 July 2024 / Published online: 13 August 2024

Abstract
We developed a cryogenic facility to assess the performance of different types of cryogenic mechanisms. The facility can host very large (up to $\sim 1\,\mathrm{m}^3$) and heavy (up to $\sim 30\,\mathrm{kg}$) instrumentation, cooled down below 10 K. The operation of moving components can be visually monitored by means of two webcams looking inside the 4 K volume. In addition a large number of electrical feedthroughs (444 lines) allow the operation of a set of hall and capacitive sensors to measure both the magnetic field, the position of moving devices with an accuracy of tens of microns and their temperatures with an accuracy of few %. We present the results of the first tests on a large aperture (500 mm diameter) superconducting magnetic bearing for the SWIPE/LSPE experiment currently under test.

Keywords Cosmology · Cryogenics · Polarization

1 Introduction

The measurement of cosmic microwave background (CMB) radiation properties (B-mode polarization, spectral distortions) probes physical phenomena near the big bang and fundamental physics at very high energy. Modern CMB experiments require large throughput detector arrays, optics and modulators, all working at cryogenic temperatures. Modulators are composed of large cryogenic mechanism which need to be carefully test to assess their performance and make a forecast of their systematics. The development of large cryogenic facilities to test the performance is the first step in its development.

✉ F. Columbro
fabio.columbro@roma1.infn.it

[1] Physics Department, Sapienza, P.le A. Moro 5, 00185 Rome, Italy

[2] INFN-Sezione di Roma1, P.le A. Moro 5, 00185 Rome, Italy

In Sec. 2 we describe the facility we developed in our laboratory while in Sec. 3 we describe the polarization modulation unit (PMU) of the SWIPE/LSPE instrument [1–3] and discuss the first tests performed. The PMU is a key and critical component [4, 5] of modern CMB experiments [6–12] which has the goal of spin a half-wave plate (HWP) optical element.

2 Cryogenic Facility

We developed a cryogenic facility to assess the performance of different types of cryogenic mechanisms. The facility (Fig. 1) can host very large (up to $\sim 1\,\mathrm{m}^3$ and heavy (up to $\sim 30\,\mathrm{kg}$) instrumentation, cooled down below 15 K. This testbed is based on a SHI pulse tube (PT) cryocooler (model RP-082B2S) with a second-stage capacity of 0.7 W. It operates with air-cooled helium compressor, and it features a separated valve unit to further reduce vibration.

Custom flexible heat straps composed of high-purity copper flanges and commercial copper wires, with an estimated thermal conductance of $\sim 0.5\ \mathrm{WK}^{-1}$, provide the connection between the second stage of the PT and the cold cryostat stage (left panel of Fig. 2).

A radiation shield surrounding the cold stage is wrapped with multilayer insulation (MLI) blanket reducing the radiative load on the first stage from ~150 W to <10 W and cooled by the first stage of the PT through a similar heat strap. The radiation shield and cold stages are supported by fiberglass tubes to provide the necessary stiffness, allowing operation of the cryostat for tilts up to 30 ° from vertical.

A large number of electrical feedthroughs (444 lines) allow the operation of multiple set of sensors. Eight thermometers monitor the temperature in different cryostat locations. A set of capacitive sensors [13] are used to monitor the displacement

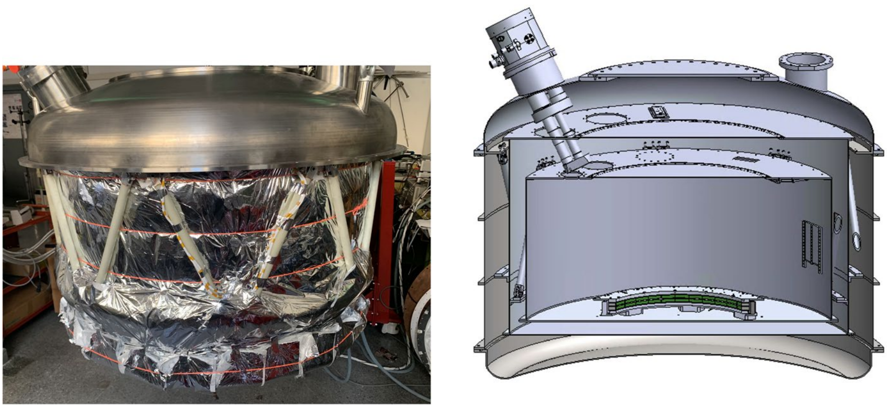

Fig. 1 Left: the cryogenic facility without the vertical section of the vacuum blanket. The radiation MLI blanket surrounds the cold stage shield. The fiberglass tubes (~ 25 mm outer diameter) provide the necessary stiffness to support the inner stages. A similar system is applied on the second stage. Right: section of the cryostat with the PMU mounted on the second stage

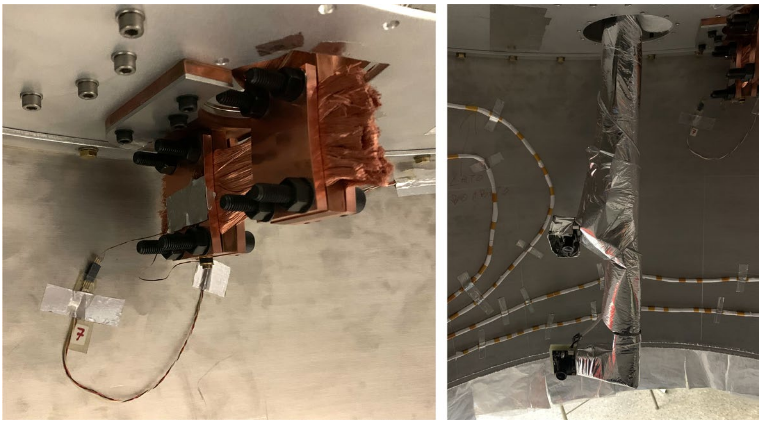

Fig. 2 Left: thermal link between the PT second stage and the inner stage of the cryostat. Right: webcams totem, connected to the first stage of the PT, and protruding inside the second-stage volume

of moving components. In addition a temperature sensor can be connected to the capacitive sensor and biased with an AC current transferred to the moving component via capacitive coupling. The position of moving devices can be monitored with an accuracy of tens of microns and their temperatures with an accuracy of few %.

The testbed is equipped with two Leopard Imaging webcams (right panel of Fig. 2). They are used to continuously monitor in real time the rotation of the system in the cryogenic environment. The webcams are attached to the first stage, looking inside the second-stage volume, and their heat load is ~1 W for each webcam (180 mA at 5 VDC).

The magnetic fields are monitored by an absolute Hall sensor (Cryomagnetics Inc.) and a set of relative Hall sensors (A sensor Technology model 144P) which can be mounted in different positions of the second-stage volume. Both sensors have a resolution of few μT.

In the current configuration, the temperature of the bottom part of the second stage, where the mechanism to be tested is located, is $\sim$ 20 K. With both webcams turned off, the equilibrium temperature is 14 K. The last region of Fig. 3 shows the effect of one webcam turned off $\sim$ 8 d after the start of the cooldown. With both webcams turned on (in order to keep them operative and warmer by self-heating), the cooling time to cooldown the second-stage plate below 30 K is $\sim$ 4 days. The equilibrium temperature reached by the second stage of the PT is 5 K. There is a non-negligible temperature gradient between the second stage of the PT and the other parts thermally connected to it, due to the thermal resistance of the flexible heat links and of the large aluminum shields. In a future implementation, we plan to improve the thermal conductivity of the heat links and to add a second pulse tube refrigerator. The cryostat has been designed and manufactured for two pulse tube refrigerators, and blank flanges are currently present in place of the second one.

In an extended version, the cryostat can also accommodate a very large focal plane. This is cooled down to sub-Kelvin temperatures by an additional pulse tube head connected to a sub-Kelvin refrigerator and can be illuminated by external

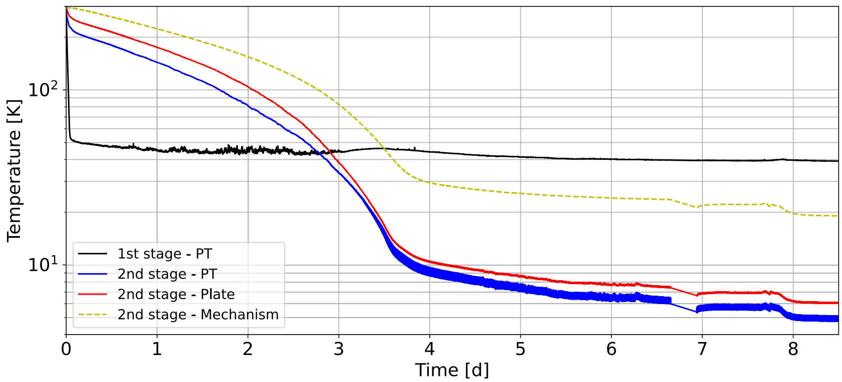

Fig. 3 Temperatures of the testbed measured in four different locations of the cryogenic testbed

radiation taking advantage of a large (∼ 600 mm diameter) optical window, followed by a stack of thermal and low-pass filters.

3 Polarization Modulation Unit Tests

The breadboard model of the polarization modulation unit (PMU) is based on the design for the SWIPE balloon-borne instrument one. This PMU is based on a 500 mm optical aperture superconductive magnetic bearing (SMB), which will host a metal-mesh HWP. Figure 4 shows the PMU ready to be tested in the cryogenic facility.

The PMU is composed of the following subsystems:

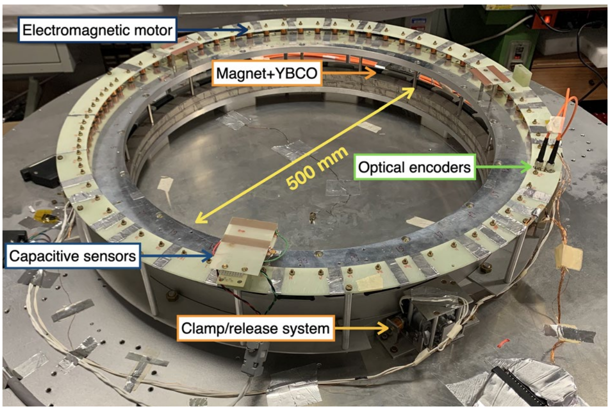

Fig. 4 The polarization modulation unit mounted on the bottom cover of the cold volume. Main components described in sec 3 are highlighted

- Bearing [14]: the SMB is composed of a stator and a rotor. A superconductor ring (18 yttrium-barium-copper-oxide tiles) in the stator and a permanent magnet ring (2 NdFeB segmented magnetic rings and 3 thin iron yokes) in the rotor are faced radially to minimize radial displacement of the SMB. The rotor includes two additional aluminum rings: the groove ring located on the bottom and coupled with the clamp/release system to hold the rotor in place at room temperature and during the cooldown; the encoder ring located on the top and including 64 slots for the relative encoder, a single slot for the absolute encoder and 8 receptacles for the small magnets which are part of the motor. The top part of the rotor can host the HWP, mounted in its custom holder.
- Clamp and Release System [15]: the rotor is held by the clamp/release mechanism, keeping it in place during the cooldown process, until the transition temperature of the YBCO bulks is reached and the magnetic field is frozen. Thereafter, the rotor is kept in place by the magnetic field, and the clamps can be released. The clamp/release mechanism is composed of three linear actuators, radially oriented toward the center of the HWP ring, spaced 120 ° in azimuth and pushing against a groove ring located below the main magnet.
- Motor [16]: an electromagnetic motor is used to spin the rotor while an optical encoder continuously monitors the position and the velocity. The electromagnetic motor is based on the interaction between 8 small (8 mm diameter, 2.5 mm height) NdFeB magnets, evenly spaced on the periphery of the rotor, and 64 driving coils placed on the same diameter on the stator. By modulating the current in each coil, we are able to simultaneously push/pull the closest magnet.
- Sensors: the performance of the PMU is monitored by means of the set of sensors previously described in the second part of Sec. 2
- Harness [17]: each of the subsystems described before needs a custom harness to be controlled and operated by the room temperature electronics. The harness is designed to minimize the heat load on the different cryogenic system stages.
- Control Electronics (at room temperature): a custom electronics controls the spin of the rotor thanks to a PID feedback control composed by the optical encoders, an Arduino board reading those, computing the error signal, applying the PID algorithm and controlling a DAC, thus generating a set of phased currents driving the coils.

The most critical parameter of such a system is its coefficient of friction which gives and estimation of the heat load produced by the bearing during its continuous rotation. It is quantified in terms of power loss, measured by spinning the rotor up and then letting it free to spin down, while reading its angular position versus time with the optical encoder. The rotation of the system is described by the equation of motion:

$$\tau(i) - \tau_f(\omega) = I\frac{d\omega}{dt} \tag{1}$$

where τ is the external torque applied to spin the rotor, τ_f is the torque of friction forces, I is the moment of inertia of the rotating system and ω the angular velocity of

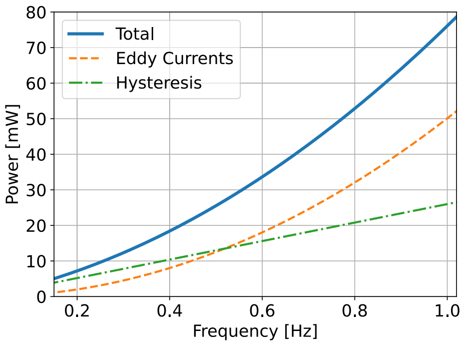

Fig. 5 Power losses measured during the spin down tests. The hysteresis and eddy current losses produced while the rotor is spinning at 30rpm are 12 mW and 13 mW, respectively

the rotor we measure. When the bearing is free to slow down (applied torque $\tau = 0$), we can write an equation for the dissipated power:

$$\tau_f(\omega) = \frac{P_f(\omega)}{\omega} \rightarrow P_f(\omega) = -\omega I \frac{d\omega}{dt} = -2\pi f I(\alpha_0 + 2\pi f \alpha_1) \tag{2}$$

where α_0 and α_1 are the coefficients of friction which come from two different contributions. Hysteresis losses (α_0) can be produced in the YBCO superconductors by the trapped magnetic field of the rotor magnet, which is not homogeneous and shifts a little bit after the release due to gravity; eddy current losses (α_1) can be induced by a time varying magnetic field ΔB and dissipate power as Joule heat (Fig. 5).

Both the main magnet and the motor magnets generate eddy currents. In order to separate the two contributions, we performed an additional test by increasing the distance between the motor magnets and the stator. The measured friction is the same in both configurations, meaning that the main contribution to eddy current losses comes from the main magnet.

4 Conclusion

We developed a cryogenic facility useful to test large mechanisms at 10 K and monitor the performance both visually thanks to cryogenic webcams and electrically by using capacitive and magnetic sensors. Currently a half meter aperture PMU is under test. The baseline rotation frequency is 30rpm, and the heat load produced is 25 mW. The large mirror transport mechanism (MTM) of the COSMO experiment [18], designed to operate at cryogenic temperature, will be tested in the next months.

Author contribution F.C. wrote the main manuscript text and co-lead the activities.P.d.B. co-lead the PMU test activity.A.C. developed the thermal links and contributed in the cryogenic facility test.S.M co-lead the cryogenic facility development activity.E.M. contributed in the PMU test activity.A.O. tested the thermal links and contributed in the cryogenic facility assembly and test.All authors reviewed the manuscript.

Funding Open access funding provided by Università degli Studi di Roma La Sapienza within the CRUI-CARE Agreement.

Declarations

Conflict of interest The authors declare no competing interests.

References

1. G. Addamo, P.A.R. Ade, C. Baccigalupi, A.M. Baldini, P.M. Battaglia, E.S. Battistelli, A. Baù, P. de Bernardis, M. Bersanelli, M. Biasotti, A. Boscaleri, B. Caccianiga, S. Caprioli, F. Cavaliere, F. Cei, K. A. Cleary, F. Columbro, G. Coppi, A. Coppolecchia, F. Cuttaia, G. D'Alessandro, G. De Gasperis, M. De Petris, V. Fafone, F. Farsian, L. Ferrari Barusso, F. Fontanelli, C. Franceschet, T. C. Gaier, L. Galli, F. Gatti, R. Genova-Santos, M. Gerbino, M. Gervasi, T. Ghigna, D. Grosso, A. Gruppuso, R. Gualtieri, F. Incardona, M. E. Jones, P. Kangaslahti, N. Krachmalnicoff, L. Lamagna, M. Lattanzi, C. H. López-Caraballo, M. Lumia, R. Mainini, D. Maino, S. Mandelli, M. Maris, S. Masi, S. Matarrese, A. May, L. Mele, P. Mena, A. Mennella, R. Molina, D. Molinari, G. Morgante, U. Natale, F. Nati, P. Natoli, L. Pagano, A. Paiella, F. Panico, F. Paonessa, S. Paradiso, A. Passerini, M. Perez-de-Taoro, O.A. Peverini, F. Pezzotta, F. Piacentini, L. Piccirillo, G. Pisano, G. Polenta, D. Poletti, G. Presta, S. Realini, N. Reyes, A. Rocchi, J.A. Rubino-Martin, M. Sandri, S. Sartor, A. Schillaci, G. Signorelli, B. Siri, M. Soria, F. Spinella, V. Tapia, A. Tartari, A.C. Taylor, L. Terenzi, M. Tomasi, E. Tommasi, C. Tucker, D. Vaccaro, D.M. Vigano, F. Villa, G. Virone, N. Vittorio, A. Volpe, R.E.J. Watkins, A. Zacchei, M. Zannoni, LSPE collaboration: the large scale polarization explorer (LSPE) for CMB measurements: performance forecast. JCAP **2021**(8), 008 (2021) https://doi.org/10.1088/1475-7516/2021/08/008 https://arxiv.org/abs/2008.11049arXiv:2008.11049 [astro-ph.IM]
2. L. Lamagna, G. Addamo, P.A.R. Ade, C. Baccigalupi, A.M. Baldini, P.M. Battaglia, E. Battistelli, A. Baù, M. Bersanelli, M. Biasotti, C. Boragno, A. Boscaleri, B. Caccianiga, S. Caprioli, F. Cavaliere, F. Cei, K.A. Cleary, F. Columbro, G. Coppi, A. Coppolecchia, D. Corsini, F. Cuttaia, G. D'Alessandro, P. de Bernardis, G. De Gasperis, M. De Petris, F.D. Torto, V. Fafone, Z. Farooqui, F. Farsian, F. Fontanelli, C. Franceschet, T.C. Gaier, F. Gatti, R. Genova-Santos, M. Gervasi, T. Ghigna, M. Grassi, D. Grosso, F. Incardona, M. Jones, P. Kangaslahti, N. Krachmalnicoff, R. Mainini, D. Maino, S. Mandelli, M. Maris, S. Masi, S. Matarrese, A. May, P. Mena, A. Mennella, R. Molina, D. Molinari, G. Morgante, F. Nati, P. Natoli, L. Pagano, A. Paiella, F. Paonessa, A. Passerini, M. Perez-de-Taoro, O.A. Peverini, F. Pezzotta, F. Piacentini, L. Piccirillo, G. Pisano, L. Polastri, G. Polenta, D. Poletti, G. Presta, S. Realini, N. Reyes, A. Rocchi, J.A. Rubino-Martin, M. Sandri, S. Sartor, A. Schillaci, G. Signorelli, M. Soria, F. Spinella, V. Tapia, A. Tartari, A. Taylor, L. Terenzi, M. Tomasi, E. Tommasi, C. Tucker, D. Vaccaro, D.M. Vigano, F. Villa, G. Virone, N. Vittorio, A. Volpe, B. Watkins, A. Zacchei, M. Zannoni, Progress report on the large-scale polarization explorer. J. Low Temp. Phys. **200**(5–6), 374–383 (2020). https://doi.org/10.1007/s10909-020-02454-x. arXiv:2005.01187 [astro-ph.IM]
3. F. Columbro, P.G. Madonia, L. Lamagna, E.S. Battistelli, A. Coppolecchia, P. de Bernardis, R. Gualtieri, S. Masi, A. Paiella, F. Piacentini, G. Presta, M. Biasotti, G. D'Alessandro, F. Gatti, L. Mele, B. Siri, SWIPE multi-mode pixel assembly design and beam pattern measurements at

cryogenic temperature. J. Low Temp. Phys. **199**(1–2), 312–319 (2020). https://doi.org/10.1007/s10909-020-02396-4
4. S. Giardiello, M. Gerbino, L. Pagano, J. Errard, A. Gruppuso, H. Ishino, M. Lattanzi, P. Natoli, G. Patanchon, F. Piacentini, G. Pisano, Detailed study of HWP non-idealities and their impact on future measurements of CMB polarization anisotropies from space. A &A **658**, 15 (2022). https://doi.org/10.1051/0004-6361/202141619. arXiv:2106.08031 [astro-ph.CO]
5. F. Columbro, E.S. Battistelli, A. Coppolecchia, G. D'Alessandro, P. de Bernardis, L. Lamagna, S. Masi, L. Pagano, A. Paiella, F. Piacentini, G. Presta, The short wavelength instrument for the polarization explorer balloon-borne experiment: polarization modulation issues. Astron. Nachr. **340**(83), 83–88 (2019). https://doi.org/10.1002/asna.201913566. arXiv:1904.01891 [astro-ph.IM]
6. LiteBIRD Collaboration, E. Allys, K. Arnold, J. Aumont, R. Aurlien, S. Azzoni, C. Baccigalupi, A.J. Banday, R. Banerji, R.B. Barreiro, N. Bartolo, L. Bautista, D. Beck, S. Beckman, M. Bersanelli, F. Boulanger, M. Brilenkov, M. Bucher, E. Calabrese, P. Campeti, A. Carones, F.J. Casas, A. Catalano, V. Chan, K. Cheung, Y. Chinone, S.E. Clark, F. Columbro, G. D'Alessandro, P. de Bernardis, T. de Haan, E. de la Hoz, M. De Petris, S.D. Torre, P. Diego-Palazuelos, M. Dobbs, T. Dotani, J.M. Duval, T. Elleflot, H.K. Eriksen, J. Errard, T. Essinger-Hileman, F. Finelli, R. Flauger, C. Franceschet, U. Fuskeland, M. Galloway, K. Ganga, M. Gerbino, M. Gervasi, R.T. Génova-Santos, T. Ghigna, S. Giardiello, E. Gjerløw, J. Grain, F. Grupp, A. Gruppuso, J.E. Gudmundsson, N.W. Halverson, P. Hargrave, T. Hasebe, M. Hasegawa, M. Hazumi, S. Henrot-Versillé, B. Hensley, L.T. Hergt, D. Herman, E. Hivon, R.A. Hlozek, A.L. Hornsby, Y. Hoshino, J. Hubmayr, K. Ichiki, T. Iida, H. Imada, H. Ishino, G. Jaehnig, N. Katayama, A. Kato, R. Keskitalo, T. Kisner, Y. Kobayashi, A. Kogut, K. Kohri, E. Komatsu, K. Komatsu, K. Konishi, N. Krachmalnicoff, C.L. Kuo, L. Lamagna, M. Lattanzi, A.T. Lee, C. Leloup, F. Levrier, E. Linder, G. Luzzi, J. Macias-Perez, T. Maciaszek, B. Maffei, D. Maino, S. Mandelli, E. Martínez-González, S. Masi, M. Massa, S. Matarrese, F.T. Matsuda, T. Matsumura, L. Mele, M. Migliaccio, Y. Minami, A. Moggi, J. Montgomery, L. Montier, G. Morgante, B. Mot, Y. Nagano, T. Nagasaki, R. Nagata, R. Nakano, T. Namikawa, F. Nati, P. Natoli, S. Nerval, F. Noviello, K. Odagiri, S. Oguri, H. Ohsaki, L. Pagano, A. Paiella, D. Paoletti, A. Passerini, G. Patanchon, F. Piacentini, M. Piat, G. Pisano, G. Polenta, D. Poletti, T. Prouvé, G. Puglisi, D. Rambaud, C. Raum, S. Realini, M. Reinecke, M. Remazeilles, A. Ritacco, G. Roudil, J.A. Rubino-Martin, M. Russell, H. Sakurai, Y. Sakurai, M. Sasaki, D. Scott, Y. Sekimoto, K. Shinozaki, M. Shiraishi, P. Shirron, G. Signorelli, F. Spinella, S. Stever, R. Stompor, S. Sugiyama, R.M. Sullivan, A. Suzuki, T.L. Svalheim, E. Switzer, R. Takaku, H. Takakura, Y. Takase, A. Tartari, Y. Terao, J. Thermeau, H. Thommesen, K.L. Thompson, M. Tomasi, M. Tominaga, M. Tristram, M. Tsuji, M. Tsujimoto, L. Vacher, P. Vielva, N. Vittorio, W. Wang, K. Watanuki, I.K. Wehus, J. Weller, B. Westbrook, J. Wilms, B. Winter, E.J. Wollack, J. Yumoto, M. Zannoni, Collaboration LiteB I R D: Probing cosmic inflation with the LiteBIRD cosmic microwave background polarization survey. Progress of Theoretical and Experimental Physics **2023**(4), 042–01 (2023) https://doi.org/10.1093/ptep/ptac150 https://arxiv.org/abs/2202.02773arXiv:2202.02773 [astro-ph.IM]
7. L. Montier, B. Mot, P. de Bernardis, B. Maffei, G. Pisano, F. Columbro, J.E. Gudmundsson, S. Henrot-Versillé, L. Lamagna, J. Montgomery, T. Prouvé, M. Russell, G. Savini, S. Stever, K.L. Thompson, M. Tsujimoto, C. Tucker, B. Westbrook, P.A.R. Ade, A. Adler, E. Allys, K. Arnold, D. Auguste, J. Aumont, R. Aurlien, J. Austermann, C. Baccigalupi, A.J. Banday, R. Banerji, R.B. Barreiro, S. Basak, J. Beall, D. Beck, S. Beckman, J. Bermejo, M. Bersanelli, J. Bonis, J. Borrill, F. Boulanger, S. Bounissou, M. Brilenkov, M. Brown, M. Bucher, E. Calabrese, P. Campeti, A. Carones, F.J. Casas, A. Challinor, V. Chan, K. Cheung, Y. Chinone, J.F. Cliche, L. Colombo, J. Cubas, A. Cukierman, D. Curtis, G. D'Alessandro, N. Dachlythra, M. De Petris, C. Dickinson, P. Diego-Palazuelos, M. Dobbs, T. Dotani, L. Duband, S. Duff, J.M. Duval, K. Ebisawa, T. Elleflot, H. K. Eriksen, J. Errard, T. Essinger-Hileman, F. Finelli, R. Flauger, C. Franceschet, U. Fuskeland, M. Galloway, K. Ganga, J.R. Gao, R. Genova-Santos, M. Gerbino, M. Gervasi, T. Ghigna, E. Gjerløw, M.L. Gradziel, J. Grain, F. Grupp, A. Gruppuso, T. de Haan, N.W. Halverson, P. Hargrave, T. Hasebe, M. Hasegawa, M. Hattori, M. Hazumi, D. Herman, D. Herranz, C. A. Hill, G. Hilton, Y. Hirota, E. Hivon, R. A. Hlozek, Y. Hoshino, E. de la Hoz, J. Hubmayr, K. Ichiki, T. Iida, H. Imada, K. Ishimura, H. Ishino, G. Jaehnig, T. Kaga, S. Kashima, N. Katayama, A. Kato, T. Kawasaki, R. Keskitalo, T. Kisner, Y. Kobayashi, N. Kogiso, A. Kogut, K. Kohri, E. Komatsu, K. Komatsu, K. Konishi, N. Krachmalnicoff, I. Kreykenbohm, C. L. Kuo, A. Kushino, J. V. Lanen, M. Lattanzi, A. T. Lee, C. Leloup, F. Levrier, E. Linder, T. Louis, G. Luzzi, T. Maciaszek, D. Maino, M. Maki, S. Mandelli, E. Martinez-Gonzalez, S. Masi, T. Matsumura,

A. Mennella, M. Migliaccio, Y. Minami, K. Mitsuda, G. Morgante, Y. Murata, J.A. Murphy, M. Nagai, Y. Nagano, T. Nagasaki, R. Nagata, S. Nakamura, T. Namikawa, P. Natoli, S. Nerval, T. Nishibori, H. Nishino, C. O'Sullivan, H. Ogawa, H. Ogawa, S. Oguri, H. Ohsaki, I. S. Ohta, N. Okada, N. Okada, L. Pagano, A. Paiella, D. Paoletti, G. Patanchon, J. Peloton, F. Piacentini, G. Polenta, D. Poletti, G. Puglisi, D. Rambaud, C. Raum, S. Realini, M. Reinecke, M. Remazeilles, A. Ritacco, G. Roudil, J.A. Rubino-Martin, H. Sakurai, Y. Sakurai, M. Sandri, M. Sasaki, D. Scott, J. Seibert, Y. Sekimoto, B. Sherwin, K. Shinozaki, M. Shiraishi, P. Shirron, G. Signorelli, G. Smecher, R. Stompor, H. Sugai, S. Sugiyama, A. Suzuki, J. Suzuki, T. L. Svalheim, E. Switzer, R. Takaku, H. Takakura, S. Takakura, Y. Takase, Y. Takeda, A. Tartari, E. Taylor, Y. Terao, H. Thommesen, B. Thorne, T. Toda, M. Tomasi, M. Tominaga, N. Trappe, M. Tristram, M. Tsuji, J. Ullom, G. Vermeulen, P. Vielva, F. Villa, M. Vissers, N. Vittorio, I. Wehus, J. Weller, J. Wilms, B. Winter, E.J. Wollack, N.Y. Yamasaki, T. Yoshida, J. Yumoto, M. Zannoni, A. Zonca, in *Overview of the medium and high frequency telescopes of the LiteBIRD space mission*, ed. by M. Lystrup, M.D. Perrin. Space Telescopes and Instrumentation 2020: Optical, Infrared, and Millimeter Wave. Society of Photo-Optical Instrumentation Engineers (SPIE) Conference Series, vol 11443 (2020), p. 114432. https://doi.org/10.1117/12.2562243

8. Y. Sakurai, P. Ashton, A. Kusaka, C.A. Hill, K. Kiuchi, N. Katayama, O. Tajima, Half-meter scale superconducting magnetic bearing for cosmic microwave background polarization experiments. J. Phys. Conf. Ser. **1590**, 012060 (2020). https://doi.org/10.1088/1742-6596/1590/1/012060
9. K. Yamada, B. Bixler, Y. Sakurai, P.C. Ashton, J. Sugiyama, K. Arnold, J. Begin, L. Corbett, S. Day-Weiss, N. Galitzki, C.A. Hill, B.R. Johnson, B. Jost, A. Kusaka, B.J. Koopman, J. Lashner, A.T. Lee, A. Mangu, H. Nishino, L.A. Page, M.J. Randall, D. Sasaki, X. Song, J. Spisak, T. Tsan, Y. Wang, P.A. Williams, The simons observatory: cryogenic half wave plate rotation mechanism for the small aperture telescopes. arXiv e-prints, 2309–14803 (2023) https://doi.org/10.48550/arXiv.2309.14803 https://arxiv.org/abs/2309.14803arXiv:2309.14803 [astro-ph.IM]
10. C.A. Hill, A. Kusaka, P. Barton, B. Bixler, A.G. Droster, M. Flament, S. Ganjam, A. Jadbabaie, O. Jeong, A.T. Lee, A. Madurowicz, F.T. Matsuda, T. Matsumura, A. Rutkowski, Y. Sakurai, D.R. Sponseller, A. Suzuki, R. Tat, A large-diameter cryogenic rotation stage for half-wave plate polarization modulation on the POLARBEAR-2 experiment. J. Low Temp. Phys. **193**(5–6), 851–859 (2018). https://doi.org/10.1007/s10909-018-1980-6. arXiv:1805.10403 [astro-ph.IM]
11. B.R. Johnson, F. Columbro, D. Araujo, M. Limon, B. Smiley, G. Jones, B. Reichborn-Kjennerud, A. Miller, S. Gupta, A large-diameter hollow-shaft cryogenic motor based on a superconducting magnetic bearing for millimeter-wave polarimetry. Rev. Sci. Instrum. **88**(10), 105102 (2017). https://doi.org/10.1063/1.4990884. arXiv:1706.05963 [astro-ph.IM]
12. A. Mennella, P. Ade, G. Amico, D. Auguste, J. Aumont, S. Banfi, G. Barbaràn, P. Battaglia, E. Battistelli, A. Baù, B. Bélier, D. Bennett, L. Bergé, J. Bernard, M. Bersanelli, M. Sazy, N. Bleurvacq, J. Bonaparte, J. Bonis, E. Bunn, D. Burke, D. Buzi, A. Buzzelli, F. Cavaliere, P. Chanial, C. Chapron, R. Charlassier, F. Columbro, G. Coppi, A. Coppolecchia, R. D'Agostino, G. D'Alessandro, P. Bernardis, G. Gasperis, M. Leo, M. Petris, A. Donato, L. Dumoulin, A. Etchegoyen, A. Fasciszewski, C. Franceschet, M. Lerena, B. Garcia, X. Garrido, M. Gaspard, A. Gault, D. Gayer, M. Gervasi, M. Giard, Y. Héraud, M. Berisso, M. González, M. Gradziel, L. Grandsire, E. Guerard, J. Hamilton, D. Harari, V. Haynes, S. Versillé, D. Hoang, N. Holtzer, F. Incardona, E. Jules, J. Kaplan, A. Korotkov, C. Kristukat, L. Lamagna, S. Loucatos, T. Louis, A. Lowitz, V. Lukovic, R. Luterstein, B. Maffei, S. Marnieros, S. Masi, A. Mattei, A. May, M. McCulloch, M. Medina, L. Mele, S. Melhuish, L. Montier, L. Mousset, L. Mundo, J. Murphy, J. Murphy, C. O'Sullivan, E. Olivieri, A. Paiella, F. Pajot, A. Passerini, H. Pastoriza, A. Pelosi, C. Perbost, M. Perciballi, F. Pezzotta, F. Piacentini, M. Piat, L. Piccirillo, G. Pisano, G. Polenta, D. Prêle, R. Puddu, D. Rambaud, P. Ringegni, G. Romero, M. Salatino, A. Schillaci, C. Scóccola, S. Scully, S. Spinelli, G. Stankowiak, M. Stolpovskiy, F. Suarez, A. Tartari, J. Thermeau, P. Timbie, M. Tomasi, S. Torchinsky, M. Tristram, C. Tucker, G. Tucker, S. Vanneste, D. Viganò, N. Vittorio, F. Voisin, R. Watson, F. Wicek, M. Zannoni, A. Zullo, QUBIC: exploring the Primordial Universe with the Q &U Bolometric Interferometer. Universe **5**(2), 42 (2019). https://doi.org/10.3390/universe5020042
13. P. de Bernardis, F. Columbro, S. Masi, A. Paiella, G. Romeo, A simple method to measure the temperature and levitation height of devices rotating at cryogenic temperatures. Rev. Sci. Instrum. **91**(4), 045118 (2020). https://doi.org/10.1063/5.0005498

14. F. Columbro, Development of the polarization modulator and multi-mode receivers for the search of CMB polarization. Memorie della SAIT **92**(1), 11 (2021)
15. F. Columbro, P. de Bernardis, S. Masi, A clamp and release system for superconducting magnetic bearings. Rev. Sci. Instrum. **89**(12), 7 (2018). https://doi.org/10.1063/1.5035332
16. F. Columbro, P. de Bernardis, L. Lamagna, S. Masi, A. Paiella, F. Piacentini, G. Pisano, in *A polarization modulator unit for the mid- and high-frequency telescopes of the LiteBIRD mission*, ed. by, M. Lystrup, M.D. Perrin, Space Telescopes and Instrumentation 2020: Optical, Infrared, and Millimeter Wave. Society of Photo-Optical Instrumentation Engineers (SPIE) Conference Series, vol 11443, p. 114436 (2020). https://doi.org/10.1117/12.2577818
17. F. Columbro, P. de Bernardis, S. Masi, Polarization modulator unit harness thermal design for the mid- and high-frequency telescopes of the LiteBIRD space mission. J. Low Temp. Phys. **211**(5–6), 407–414 (2023). https://doi.org/10.1007/s10909-022-02919-1. arXiv:2101.05188 [astro-ph.IM]
18. L. Mele, E.S. Battistelli, P. de Bernardis, M. Bersanelli, F. Columbro, G. Coppi, A. Coppolecchia, G. D'Alessandro, M. De Petris, C. Franceschet, M. Gervasi, L. Lamagna, A. Limonta, E. Manzan, E. Marchitelli, S. Masi, A. Mennella, F. Nati, A. Paiella, G. Pettinari, F. Piacentini, L. Piccirillo, G. Pisano, S. Realini, C. Tucker, M. Zannoni, Measuring CMB spectral distortions from antarctica with COSMO: blackbody calibrator design and performance forecast. J. Low Temp. Phys. **209**(5–6), 912–918 (2022). https://doi.org/10.1007/s10909-022-02874-x